A variable-temperature X-ray diffraction and theoretical study of conformational polymorphism in a complex organic molecule (DTC)

Andrea Gionda,[a] Giovanni Macetti,[a,b] Laura Loconte,[a] Silvia Rizzato,[a] Ahmed M. Orlando,[a] Carlo Gatti,[b,c] Leonardo Lo Presti*[,a,b,c]

[a] Università degli Studi di Milano, Department of Chemistry, Via Golgi 19 I-20133 Milano (Italy)

[b] Centre for Materials Crystallography, Århus University, Langelandsgade 140, DK-8000 Århus C. (Denmark)

[c] Istituto di Scienze e Tecnologie Molecolari, Italian CNR, Via Golgi 19 I-20133 Milano (Italy)

To whom correspondence should be addressed: leonardo.lopresti@unimi.it

ELECTRONIC SUPPLEMENTARY INFORMATION

S1. Details of the energy decomposition schemes explored in this work

See Section 2.7 in the main text for a general introduction.

CE-B3LYP. The B3LYP/6-31G(d,p) theory level was employed throughout to estimate Coulombic and repulsive terms between molecular pairs in structures A and B at T = 100 K. Dispersive potentials and polarization energies were estimated with the semiempirical functionals described by Thomas et al..[1] The program focuses on the symmetry-independent molecule, and computes pair interaction energies with all the neighbouring molecules within a user-defined distance cutoff. As for the present calculations, molecules exhibiting atom-atom contact distances lower than 14 Å with respect to the reference one in the asymmetric unit were included, corresponding to a maximum of centre-of-mass distance of ~ 24 Å, for a total of either 71 (form A) or 70 pairs at increasing distances. Such calculations are quite costly when applied to DTC, with more than 160 atoms in the reference unit cell. The CE-B3LYP method is fully implemented in CrystalExplorer17 software.[2]

PIXEL calculations. The PIXEL approach, as implemented in the CLP-PIXEL suite of programs,[3,4] uses semiempirical terms, calibrated onto experimental thermochemical data of real crystal structures, to estimate E_{p}, E_{dis} and E_{rep}, while the Coulomb energy is obtained by summation over interacting grids of charge density pixels derived from MP2/6–31G(d,p) wavefunctions. Charge densities of symmetry–independent molecules at their frozen in–crystal (TLS+H)-corrected experimental geometries (see Section 2.3 in the main text) were computed by the Gaussian09 package.[5] The usual grid condensation factor of 4 was used throughout.

AA-CLP calculations. Default program settings[6] were considered for these calculations, with a 40 Å distance cutoff for including atom-atom contributions into the lattice sums. As above, (TLS+H)-corrected experimental geometries were used.

ECDA calculations. For each crystal form in the 100 K – RT range, we first computed the M06/*pob*-TZVP wavefunction (Section 2.4 in the main text) of the isolated molecule, with geometry fixed at the in-crystal (TLS+H)-corrected experimental estimate (Section 2.3 in the main text). Then, a model of the crystal was reconstructed by applying to the wavefunction-derived charge density of the asymmetric unit the symmetry elements of the $P21/n$ space group. The program[7] considers interactions of the symmetry-independent reference molecule with all its symmetry-dependent images within a cluster of 3^3 unit cells around the reference crystallographic cell. Within this cluster, interaction energies are evaluated as a sum of atom-atom contributions, according to

$$E_{\text{tot}} = E_{\text{el}} + E_{\text{dis}} + E_{\text{rep}} \tag{ES1}$$

With E_{tot} being either E_{coh} or E_{int} (see Section 2.7 in the main text). Electrostatic terms were computed by means of the Spackman's ECDA method[8,9] (see also Section 2.7 in the main text). This means that the total electrostatic energy, E_{el}, is expressed as a sum of promolecule-promolecule, promolecule-deformation and deformation-deformation terms, according with:

$$E_{\text{el}} = E_{\text{pro-pro}} + E_{\text{pro-def}} + E_{\text{def-def}} \tag{ES2}$$

Here, $E_{\text{pro-pro}}$ is computed as a sum of Coulombic contributions between pairs of spherical atoms. $E_{\text{pro-def}}$ takes into account penetration of the deformation density of one molecule with the spherical part of the one to which it is interacting. Eventually, $E_{\text{def-def}}$ accounts for the interaction among atom-centred point multipoles up to l = 4 order of the spherical harmonic functions, and it is computed in terms of Cartesian tensor formulation of Buckingham.[10]

E_{el} is the most critical term in the summation, as it depends on Coulomb terms that fade away very slowly with distance, especially in a strongly polar structure like DTC. Therefore, convergence of electrostatic sums was verified against both the intermolecular centre-of-mass distance (Figure S1) and the order of the multipole expansion in the distributed multipole analysis (DMA). A maximum order of 4 for higher multipoles is sufficient to ensure convergence of the $E_{\text{def-def}}$ contribution.

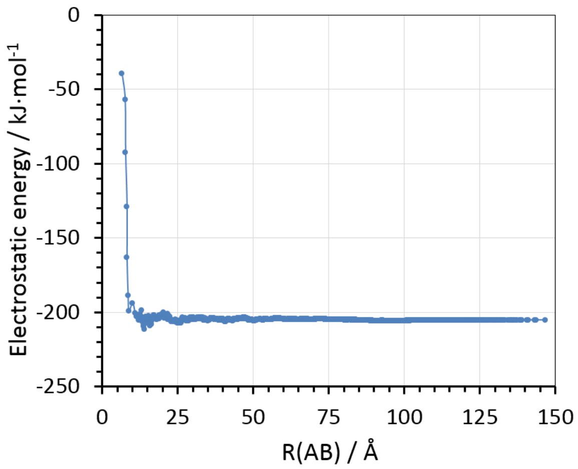

Figure S1. ECDA-derived electrostatic energies, as a function of the molecular centre-of-mass distances in the cluster employed to evaluate energy sums. The blue line serves only as a guide for the eye. As an example, results for the polymorph A structure at $T = 100$ K are here reported. Other structures show an analogue behaviour.

The contributions of 8188 additional molecular pairs out of the main cluster of 27 crystallographic unit cells were taken into account using their central moments. This always resulted in minor corrections to the electrostatic energy (<1 kJ·mol^{-1}), further confirming that the sums over electrostatic energies are fully converged above a intermolecular separation of ~ 40–50 Å (Figure S1).

The dispersive-repulsive sums $E_{\text{dis}} + E_{\text{rep}}$ are computed through *ad hoc* functionals. In particular, the following ones were considered for the set of Dispersion Atomic Parameters (DAP) required for calculation of atom-atom dispersion interaction energies:

(1) Slater-Kirkwood (SK) parameters,[11] which include refined atomic polarizabilities (see *infra*).
(2) Wu-Yang-corrected SK (WYSK) parameters,[12] including refined atomic polarizabilities (see *infra*).

Atomic polarizabilities and C_6 parameters were refined with a least-squares procedure against a set of 87 intermolecular C_6 coefficients: 77 from experimental dipole oscillator strength distributions (DOSD's)[7] and 10 from ab-initio CCSD(T)/aug-cc-pVDZ and time-dependent Hartree-Fock response theory calculations of nucleic acid base pairs.[13]

In addition, the following dampening function were considered in conjunction with the Dispersion Atomic Parameters above listed:

(1) Tang-Toennies (TT) damping function,[14] where the damping parameter D_0 is expressed by the sum of atomic Born-Mayer repulsion parameters B_i and B_j.
(2) Wu and Yang Fermi-like damping function (WY),[7,12] with corrections suggested by Grimme.[15]
(3) No damping (ND).

As for the repulsive part of the potential (exchange-repulsion energy E_{rep}), the following functionals were considered:

(1) Spackman's parameters (S).[16]
(2) Modified S parameters to fit Ziegler-Rauk ADF-BLYP/TZP repulsion energies (SZR).[7,17]

(3) Least-squares refined atomic parameters, which fit Ziegler-Rauk ADF-BLYP/TZP repulsion energies (RZR).[7,17]

Figure S2 compares the ability of different combinations of ECDA functionals in reproducing the benchmark M06/*pob*-TZVP estimates for the molecule-molecule interaction energies, E_{int}, as a function of the centre of mass distance in both polymorphs at T = 100 K.

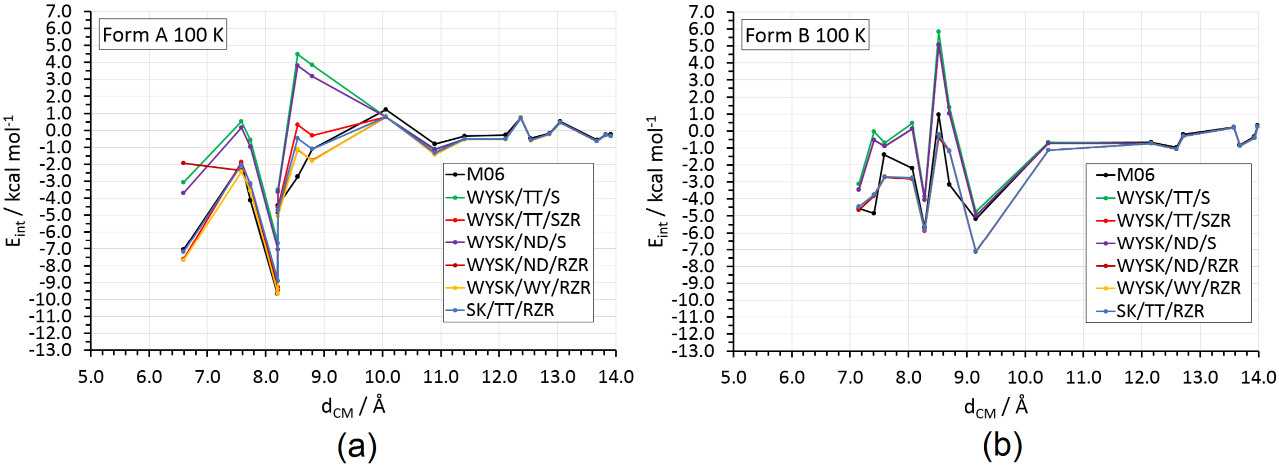

Figure S2. ECDA-derived molecule-molecule pairwise interaction energies, compared with BSSE-corrected M06/*pob*-TZVP quantum calculations at the in-crystal experimental geometries. Results of polymorph A (a) and B (b) are shown, both referring to the 100 K structures. The curves are labelled as XX/YY/ZZ, where XX indicates the dispersion functional, YY the dampening function and ZZ the exchange-repulsion functional, according with definitions given above. M06 stands for full quantum simulations.

Molecule-molecule interaction energies, E_{int}, for M1···M2 isolated molecular pairs up to a centre-of-mass distance of 14 Å in both polymorphs were also computed with Gaussian09[5] at the same M06/*pob*–TZVP level of theory used for solid-state calculations (see Section 2.6 in the main text) according to

$$E_{\text{int}} = E_{\text{pair}} - E_{\text{mol}}(\text{M1}) - E_{\text{mol}}(\text{M2}) + \Delta E_{\text{BSSE}} \quad \text{(ES3)}$$

E_{pair} is the electronic energy eigenvalue of the whole pair, E_{mol}(M1) and E_{mol}(M2) the corresponding energies of isolated M1 and M2 molecules at the same (TLS+H) in-crystal geometry, and ΔE_{BSSE} the BSSE correction.

As expected, the agreement with M06 estimates is quite good at large distances, when interaction energies become lower and lower, while it becomes necessarily worse at short d_{CM}, where local deformations of the interacting charge densities and penetration effects are not negligible. The correct definition of the exchange-repulsion functional is crucial, as it can be appreciated in Figure S2. Both S and SZR recipes somewhat overestimate E_{rep} of short contacts, while the RZR functional allows a much higher agreement with quantum simulations for both polymorphs. However, while in the B form the results are essentially independent from the choice of the dispersion functional and its dampening scheme (Figure S2b), in the A form the WYSK/WY/RZR combination is the best performing one. Actually, its corresponding root-mean-square-deviation (RMSD) with respect to the reference M06 curve was as low as 0.52 kcal·mol^{-1} (form A) and 0.93 kcal·mol^{-1} (form B). Thus, in the main text we focus the discussion just on this latter one.

Comparison of ECDA outcomes with those from other methods are discussed in the main text (Sections 3.7 and 3.8).

S2. Multi-T analysis

Table S1. Crystallographic and refinement details of the phase A of DTC. Empirical formula: $C_{14}H_{17}SO_3N_3$. Molecular weight: 307.37 a.m.u.. Lattice (all structures) monoclinic, $P2_1/n$. Z, Z'[1] = 4, 1. F(000) = 648. Crystallization solvent: Et_2O: CH_2Cl_2 1:1. Crystal size: 0.150 x 0.175 x 0.275 mm^3.

Temperature / K	100	120	140	180	220	260	292
Crystal data							
a / Å	8.5429(1)	8.5506(1)	8.5570(1)	8.5732(1)	8.5912(1)	8.6122(1)	8.6335(2)
b / Å	13.2378(2)	13.2506(2)	13.2608(2)	13.2867(2)	13.3150(2)	13.3460(2)	13.3739(3)
c / Å	13.0463(2)	13.0615(2)	13.0750(2)	13.1056(2)	13.1382(2)	13.1742(2)	13.2075(2)
β / deg	95.0916(6)	95.0620(7)	95.0428(7)	94.9773(7)	94.8947(7)	94.7854(8)	94.6615(9)
V /Å^3	1469.57(5)	1474.10(6)	1477.93(6)	1487.23(6)	1497.42(6)	1508.93(6)	1519.95(7)
Density / g·cm^{-3}	1.389	1.385	1.381	1.373	1.363	1.353	1.343
μ / mm^{-1}	0.234	0.233	0.233	0.231	0.23	0.228	0.226
Data collection							
Measured reflns	21351	22149	22262	22412	22590	22822	23025
Unique reflns.	3383	3393	3403	3429	3451	3489	3498
Obs. (I>2σ(I)) unique reflns	2923	2918	2897	2871	2839	2779	2721
Completeness	0.999	0.999	0.999	1.000	0.999	0.998	1.000
R_{int}	0.0264	0.0275	0.0280	0.0280	0.0291	0.0304	0.0308
Refinement							
Max resolution / Å	0.768	0.768	0.768	0.768	0.769	0.768	0.770
$R(F)$, I > 2 σ(I)	0.0359	0.0360	0.0359	0.0369	0.0378	0.0391	0.0413
$R(F)$, all	0.0430	0.0433	0.0434	0.0455	0.0473	0.0518	0.0565
Goodness-of-fit	1.026	1.044	1.026	1.009	1.010	1.017	0.992
$\Delta\rho_{MAX}$, / e·Å^{-3}	0.349	0.336	0.345	0.327	0.279	0.282	0.272
$\Delta\rho_{MIN}$ / e · Å^{-3}	-0.342	-0.317	-0.314	-0.302	-0.265	-0.253	-0.254

[1] Z: number of molecular formulae in the unit cell. Z': number of formula units in the asymmetric unit.

Table S2. Crystallographic and refinement details of the phase B of DTC. Empirical formula: $C_{14}H_{17}SO_3N_3$. Molecular weight: 307.37 a.m.u.. Lattice (all structures) monoclinic, $P2_1/n$. Z, Z'[2] = 4, 1. F(000) = 648. Crystallization solvent: water. Crystal size:180 x 0.160 x 0.160 mm^3.

Temperature / K	100	120	140	180	220	260	297
Crystal data							
a / Å	8.2765(1)	8.2852(1)	8.2946(1)	8.3144(1)	8.3365(1)	8.3607(2)	8.3830(2)
b / Å	17.2288(3)	17.2551(3)	17.2836(3)	17.3484(3)	17.4149(3)	17.4896(3)	17.5599(3)
c / Å	10.3944(2)	10.3985(2)	10.4035(2)	10.4141(2)	10.4268(2)	10.4410(2)	10.4546(2)
β / deg	94.9855(6)	94.9870(7)	94.9878(7)	94.9784(7)	94.9907(8)	95.0136(8)	95.0400(9)
V /Å^3	1476.58(6)	1480.95(6)	1485.79(6)	1496.46(6)	1508.02(7)	1520.90(7)	1533.01(7)
Density / g·cm^{-3}	1.383	1.379	1.374	1.364	1.354	1.342	1.332
μ / mm^{-1}	0.233	0.232	0.231	0.230	0.228	0.226	0.224
Data collection							
Measured reflns	22043	22108	22216	22359	22543	22741	22950
Unique reflns.	3410	3418	3427	3462	3489	3511	3534
Obs. (I>2σ(I)) unique reflns	2846	2830	2813	2743	2672	2548	2390
Completeness	0.999	1.000	1.000	1.000	1.000	1.000	0.999
R_{int}	0.0284	0.0289	0.0296	0.0295	0.0304	0.0322	0.0331
Refinement							
Max resolution / Å	0.769	0.769	0.769	0.768	0.768	0.768	0.769
$R(F)$, $I > 2\ \sigma(I)$	0.0358	0.0358	0.0366	0.0373	0.0394	0.0407	0.0430
$R(F)$, all	0.0451	0.0460	0.0466	0.0504	0.0559	0.0610	0.0702
Goodness-of-fit	1.006	1.018	0.990	1.004	0.993	0.989	0.988
$\Delta\rho_{MAX}$, / e·Å^{-3}	0.321	0.272	0.251	0.229	0.240	0.224	0.186
$\Delta\rho_{MIN}$ / e · Å^{-3}	-0.379	-0.410	-0.405	-0.345	-0.363	-0.328	-0.319

[2] Z: number of molecular formulae in the unit cell. Z': number of formula units in the asymmetric unit.

Table S3. Eigenvalues of the translations (t_1, t_2 and t_3) and libration (α_1, α_2 and α_3) tensors describing the rigid body motion of the DTC asymmetric unit in the form A as a function of temperature, as retrieved by the Schomaker & Trueblood TLS decomposition. Values are given in Å^2 and deg^2 and refer to the molecular inertial reference system.

T / K	100	120	140	180	220	260	292
t_1	0.01787	0.01998	0.02203	0.02715	0.03261	0.03912	0.04561
t_2	0.01522	0.01657	0.01798	0.02137	0.02544	0.02959	0.03405
t_3	0.01321	0.01435	0.01610	0.01968	0.02325	0.02726	0.03163
α_1	3.98	4.93	5.68	7.33	9.30	11.83	13.48
α_2	2.06	2.49	2.82	3.62	4.72	5.83	6.91
α_3	0.91	1.06	1.33	1.79	2.34	2.98	3.81

Table S4. Same as Table S3, for the asymmetric unit of the B polymorph.

T / K	100	120	140	180	220	260	297
t_1	0.02093	0.02324	0.02578	0.03176	0.03794	0.04501	0.05202
t_2	0.01927	0.02163	0.02378	0.02951	0.03471	0.04102	0.04724
t_3	0.01601	0.01768	0.01946	0.02349	0.02842	0.03395	0.03963
α_1	5.27	6.32	7.47	9.75	12.43	15.23	17.91
α_2	1.83	2.17	2.52	3.23	4.06	4.83	5.83
α_3	1.09	1.37	1.56	2.24	2.86	3.7	4.61

Table S5. TLS+H corrected fractional coordinates (dimensionless) as a function of *T*, for the DTC A form.

T / K	100			120			140			180			220			260			292		
Atom	X	Y	Z	X	Y	Z	X	Y	Z	X	Y	Z	X	Y	Z	X	Y	Z	X	Y	Z
S1	0.167940	0.560931	0.711042	0.167923	0.560785	0.710959	0.167987	0.560663	0.710876	0.168044	0.560415	0.710740	0.167988	0.560056	0.710560	0.167871	0.559664	0.710381	0.167594	0.559293	0.710258
C1	-0.226625	1.037969	0.603599	-0.226275	1.037897	0.603623	-0.225792	1.037642	0.603652	-0.225076	1.037178	0.603837	-0.223937	1.036827	0.603828	-0.222998	1.036251	0.603906	-0.222204	1.035650	0.604129
C10	0.174394	0.556120	0.497083	0.174485	0.556212	0.497214	0.174388	0.556302	0.497418	0.174376	0.556473	0.497725	0.174658	0.556784	0.498104	0.174795	0.557074	0.498575	0.175008	0.557360	0.498973
C11	0.622128	0.692058	0.656633	0.621702	0.692018	0.656643	0.621288	0.691735	0.656661	0.620180	0.691519	0.656666	0.619425	0.691259	0.656628	0.618177	0.690862	0.656888	0.616911	0.690505	0.656839
C12	0.627124	0.786299	0.722582	0.626985	0.785708	0.722713	0.626897	0.785269	0.722933	0.626388	0.784125	0.723499	0.625877	0.783134	0.723908	0.624917	0.781892	0.724211	0.624628	0.780489	0.724811
C13	0.458385	0.723633	0.488707	0.457993	0.723704	0.488939	0.457873	0.723824	0.489332	0.457575	0.723945	0.489985	0.457135	0.724051	0.490574	0.456668	0.724134	0.491404	0.455761	0.724234	0.492439
C14	0.527131	0.652629	0.412571	0.526811	0.652817	0.412900	0.526674	0.653108	0.413301	0.525814	0.653467	0.413989	0.525333	0.654117	0.414539	0.524654	0.654799	0.415453	0.523997	0.655465	0.416066
C2	-0.116997	0.886218	0.541394	-0.116765	0.886069	0.541726	-0.116288	0.885853	0.541966	-0.115682	0.885529	0.542601	-0.114521	0.885118	0.543269	-0.113332	0.884740	0.544190	-0.112023	0.884193	0.545168
C3	-0.134457	0.805838	0.472003	-0.134082	0.805792	0.472372	-0.133530	0.805764	0.472712	-0.132524	0.805602	0.473244	-0.131079	0.805636	0.474015	-0.129558	0.805577	0.474973	-0.128246	0.805750	0.475753
C4	-0.035715	0.723025	0.484062	-0.035355	0.722905	0.484393	-0.034957	0.722956	0.484555	-0.034377	0.723069	0.485259	-0.033635	0.723112	0.485955	-0.032796	0.723146	0.486769	-0.031893	0.723309	0.487701
C5	0.006259	0.886619	0.618852	0.006303	0.886403	0.619117	0.006204	0.886039	0.619349	0.006004	0.885279	0.619888	0.005949	0.884592	0.620666	0.005925	0.883829	0.621365	0.006227	0.883036	0.622480
C6	0.106141	0.803526	0.629471	0.105930	0.803366	0.629696	0.105728	0.803021	0.629921	0.104972	0.802406	0.630541	0.104674	0.801798	0.631194	0.103968	0.801178	0.631928	0.103743	0.800546	0.632944
C7	0.083908	0.720493	0.564152	0.083810	0.720366	0.564286	0.083771	0.720278	0.564561	0.083704	0.719983	0.565110	0.083791	0.719699	0.565777	0.083585	0.719587	0.566449	0.083660	0.719364	0.567199
C8	0.183658	0.627152	0.583357	0.183495	0.627138	0.583574	0.183543	0.627048	0.583641	0.183459	0.627104	0.583925	0.183352	0.626865	0.584258	0.183255	0.626931	0.584609	0.183072	0.626875	0.585102
C9	0.351138	0.639818	0.634666	0.350952	0.639811	0.634761	0.350938	0.639785	0.634927	0.350340	0.639742	0.634946	0.349873	0.639637	0.635078	0.349268	0.639498	0.635245	0.348014	0.639282	0.635373
H11A	0.716999	0.694765	0.605847	0.716433	0.694867	0.605853	0.715925	0.694559	0.605885	0.714435	0.694680	0.605807	0.713268	0.694780	0.605673	0.711815	0.694484	0.605993	0.709861	0.694485	0.605631
H11B	0.640075	0.625665	0.705952	0.639665	0.625526	0.705663	0.638919	0.625178	0.705492	0.637756	0.624661	0.704750	0.636997	0.624196	0.704062	0.635370	0.623767	0.703926	0.633962	0.623043	0.702979
H12A	0.739117	0.790812	0.767277	0.738978	0.789973	0.767222	0.738793	0.789271	0.767412	0.738240	0.787589	0.767629	0.737581	0.786217	0.767736	0.736330	0.784564	0.767813	0.736011	0.782491	0.767866
H12B	0.610867	0.851775	0.673799	0.610673	0.851234	0.674158	0.610776	0.850898	0.674633	0.610182	0.849983	0.675848	0.609423	0.849125	0.676815	0.608768	0.847974	0.677603	0.608223	0.846806	0.678931
H12C	0.534462	0.782992	0.773331	0.534504	0.782239	0.773495	0.534457	0.781802	0.773659	0.534268	0.780260	0.774252	0.534030	0.778849	0.774641	0.533158	0.777416	0.774790	0.533322	0.775649	0.775519
H13A	0.520068	0.795894	0.488923	0.519417	0.795967	0.489141	0.519273	0.796030	0.489688	0.519254	0.795877	0.490518	0.518444	0.795923	0.491290	0.517827	0.795846	0.492362	0.516314	0.795964	0.493680
H13B	0.334816	0.737440	0.463803	0.334511	0.737421	0.464131	0.334512	0.737532	0.464506	0.334579	0.737999	0.465263	0.334371	0.737991	0.466080	0.334269	0.738140	0.467077	0.333550	0.737980	0.468554
H14A	0.515199	0.686157	0.337065	0.514709	0.686294	0.337479	0.514614	0.686569	0.337965	0.514032	0.687138	0.338962	0.513416	0.688075	0.339880	0.512879	0.688981	0.341155	0.511896	0.689929	0.342146
H14B	0.649552	0.639846	0.436153	0.649119	0.640167	0.436500	0.648861	0.640436	0.436904	0.647644	0.640433	0.437484	0.646857	0.641133	0.437988	0.645815	0.641834	0.438819	0.644878	0.642640	0.439170
H14C	0.464844	0.581835	0.411036	0.464763	0.582027	0.411440	0.464675	0.582369	0.411771	0.463411	0.583055	0.412334	0.463175	0.583811	0.412786	0.462548	0.584690	0.413499	0.462286	0.585414	0.413988
H1A	-0.319686	1.090980	0.582766	-0.319154	1.090850	0.582596	-0.318562	1.090550	0.582588	-0.317458	1.089990	0.582416	-0.316002	1.089480	0.582112	-0.314508	1.088800	0.581710	-0.313086	1.088110	0.581376
H1B	-0.244145	1.004340	0.676879	-0.244013	1.004460	0.676859	-0.243603	1.004190	0.676783	-0.243803	1.003740	0.676632	-0.242872	1.003510	0.676444	-0.243137	1.003040	0.676149	-0.243344	1.002400	0.675988
H1C	-0.114964	1.076250	0.608563	-0.114636	1.076040	0.608668	-0.114178	1.075680	0.608736	-0.113510	1.074950	0.609360	-0.112471	1.074340	0.609347	-0.111615	1.073430	0.610059	-0.110997	1.072590	0.610796
H3	-0.225352	0.808316	0.408669	-0.224841	0.808232	0.409110	-0.224208	0.808229	0.409530	-0.222578	0.808143	0.410013	-0.220511	0.808400	0.410784	-0.218325	0.808561	0.411781	-0.216216	0.809054	0.412533
H4	-0.051306	0.659999	0.431215	-0.050748	0.659909	0.431638	-0.050001	0.660146	0.431665	-0.049243	0.660476	0.432376	-0.048379	0.660699	0.433154	-0.047281	0.660975	0.433997	-0.046147	0.661295	0.435037
H5	0.024087	0.950732	0.670126	0.024216	0.950387	0.670403	0.023967	0.949863	0.670736	0.023696	0.948803	0.671372	0.023056	0.947690	0.672429	0.022813	0.946651	0.673145	0.022743	0.945521	0.674393
H6	0.202517	0.803298	0.689290	0.202089	0.803020	0.689500	0.201630	0.802588	0.689768	0.200084	0.801713	0.690586	0.199323	0.800937	0.691169	0.197759	0.800012	0.692028	0.196917	0.798999	0.692996
N1	0.470416	0.682697	0.594026	0.470114	0.682781	0.594175	0.469964	0.682765	0.594274	0.469034	0.682921	0.594560	0.468475	0.682950	0.594828	0.467549	0.682931	0.595237	0.466678	0.682906	0.595699
N2	0.352963	0.598881	0.727865	0.352847	0.598686	0.727835	0.352682	0.598694	0.727585	0.352200	0.598326	0.727343	0.351720	0.598012	0.727010	0.350903	0.597741	0.726771	0.350014	0.597220	0.726711
N3	0.169736	0.499712	0.430244	0.169683	0.499922	0.430423	0.169922	0.500173	0.430767	0.170035	0.500576	0.431222	0.170328	0.501172	0.431786	0.170874	0.501644	0.432405	0.171505	0.502269	0.433048
O1	-0.227907	0.960282	0.526903	-0.227222	0.960045	0.527133	-0.226733	0.959908	0.527291	-0.225332	0.959617	0.527771	-0.223904	0.959173	0.528143	-0.221947	0.958927	0.528785	-0.220024	0.958677	0.529591
O2	0.156060	0.452736	0.702966	0.156135	0.452748	0.702680	0.156273	0.452790	0.702506	0.156489	0.452825	0.702097	0.156757	0.452748	0.701563	0.157022	0.452661	0.701159	0.156984	0.452538	0.700549
O3	0.067504	0.612675	0.775840	0.067551	0.612357	0.775778	0.067687	0.612131	0.775705	0.068037	0.611387	0.775551	0.068341	0.610605	0.775476	0.068294	0.609722	0.775387	0.068186	0.608866	0.775322

Table S6. TLS+H corrected fractional coordinates (dimensionless) as a function of *T*, for the DTC B form.

T / K	100			120			140			180			220			260			297		
Atom	X	Y	Z	X	Y	Z	X	Y	Z	X	Y	Z	X	Y	Z	X	Y	Z	X	Y	Z
S1	0.970259	0.801459	0.398371	0.970098	0.801458	0.398344	0.969969	0.801428	0.398302	0.969624	0.801382	0.398238	0.969223	0.801324	0.398270	0.968926	0.801322	0.398404	0.968699	0.801229	0.398465
C1	0.749662	1.067479	-0.147205	0.749628	1.067249	-0.146864	0.749628	1.066905	-0.146590	0.749471	1.066486	-0.146010	0.749570	1.065782	-0.145267	0.749262	1.065228	-0.144423	0.749256	1.064563	-0.143332
C10	0.823141	0.933233	0.496190	0.823309	0.933078	0.496283	0.823417	0.932824	0.496012	0.823514	0.932228	0.496040	0.823715	0.931756	0.495966	0.824043	0.931177	0.496036	0.824460	0.930375	0.495809
C11	0.479786	0.720987	0.454738	0.480072	0.721160	0.454500	0.480705	0.721112	0.454279	0.481419	0.721479	0.453893	0.482419	0.721639	0.453479	0.483584	0.721884	0.453049	0.484442	0.722140	0.452509
C12	0.423913	0.688556	0.322398	0.424315	0.688669	0.322388	0.424583	0.688833	0.322327	0.425167	0.689211	0.322506	0.425707	0.689649	0.322772	0.426181	0.690042	0.323268	0.426610	0.690597	0.323509
C13	0.458601	0.867385	0.465429	0.458687	0.867192	0.465113	0.458963	0.867028	0.464656	0.459567	0.866762	0.463904	0.459957	0.866506	0.462958	0.460676	0.866122	0.462125	0.461375	0.865902	0.461157
C14	0.451194	0.883378	0.608981	0.451182	0.883382	0.608286	0.450737	0.883326	0.607598	0.450212	0.883105	0.606459	0.450070	0.882776	0.605219	0.449623	0.882841	0.603615	0.448979	0.882597	0.602175
C2	0.707809	0.971849	0.011421	0.707757	0.971688	0.011786	0.708191	0.971535	0.012029	0.708555	0.971188	0.012528	0.709136	0.970844	0.013150	0.709325	0.970435	0.013857	0.710012	0.970051	0.014593
C3	0.787840	1.016054	0.108954	0.787564	1.015792	0.109158	0.787447	1.015669	0.109389	0.787056	1.014963	0.109916	0.786732	1.014453	0.110633	0.786163	1.013739	0.111296	0.786264	1.013041	0.112105
C4	0.815433	0.985246	0.232880	0.815178	0.985063	0.232940	0.814999	0.984808	0.232972	0.814631	0.984327	0.233502	0.814065	0.983821	0.233764	0.813435	0.983180	0.234185	0.812976	0.982763	0.234581
C5	0.650567	0.897908	0.039114	0.651107	0.897836	0.039296	0.651620	0.897852	0.039445	0.652849	0.897730	0.039717	0.654061	0.897686	0.040130	0.655355	0.897555	0.040527	0.656709	0.897456	0.040979
C6	0.678610	0.867651	0.162120	0.679211	0.867657	0.162007	0.679473	0.867572	0.161888	0.680583	0.867534	0.161922	0.681634	0.867455	0.161919	0.682976	0.867456	0.161904	0.684172	0.867338	0.162101
C7	0.761985	0.911125	0.260234	0.762173	0.910990	0.260290	0.762314	0.910925	0.260368	0.762492	0.910548	0.260551	0.762999	0.910373	0.260655	0.763396	0.909979	0.260917	0.763788	0.909717	0.260997
C8	0.804295	0.875874	0.392485	0.804217	0.875877	0.392459	0.804030	0.875791	0.392350	0.804327	0.875597	0.392227	0.804480	0.875213	0.392048	0.804593	0.875061	0.392041	0.804806	0.874727	0.392202
C9	0.710405	0.802045	0.422876	0.710503	0.802248	0.422756	0.710696	0.802121	0.422762	0.710890	0.802222	0.422692	0.711285	0.802382	0.422562	0.711582	0.802408	0.422485	0.711938	0.802611	0.422500
H11A	0.375868	0.726397	0.512057	0.376260	0.726637	0.511774	0.377247	0.726430	0.511814	0.378447	0.726874	0.511617	0.380197	0.726882	0.511658	0.382167	0.727158	0.511646	0.383781	0.727375	0.511510
H11B	0.566399	0.680990	0.504568	0.566544	0.681222	0.504365	0.567474	0.681275	0.503743	0.568159	0.681890	0.503332	0.569547	0.682303	0.502389	0.570842	0.682748	0.501535	0.571880	0.683172	0.500483
H12A	0.368404	0.632677	0.333338	0.368908	0.632882	0.333501	0.369432	0.633093	0.333439	0.370318	0.633677	0.333987	0.371425	0.634247	0.334409	0.372262	0.634876	0.335337	0.373129	0.635615	0.335839
H12B	0.337462	0.727737	0.273806	0.338046	0.727811	0.273756	0.338192	0.727948	0.274080	0.338950	0.728193	0.274393	0.339395	0.728525	0.275211	0.339983	0.728838	0.276138	0.340409	0.729300	0.276867
H12C	0.526854	0.682533	0.266526	0.527242	0.682605	0.266658	0.527136	0.682963	0.266293	0.527399	0.683340	0.266439	0.527357	0.684062	0.266384	0.527147	0.684493	0.266560	0.526969	0.685273	0.266495
H13A	0.335972	0.858850	0.419868	0.336209	0.858440	0.419669	0.336810	0.858256	0.418882	0.338052	0.857992	0.417529	0.339002	0.857673	0.416213	0.340372	0.857063	0.414990	0.341815	0.856906	0.413213
H13B	0.511285	0.917436	0.420002	0.511090	0.917127	0.419426	0.511523	0.916851	0.419070	0.512488	0.916328	0.418522	0.513053	0.915830	0.417729	0.513665	0.915212	0.416943	0.514790	0.914746	0.416346
H14A	0.378775	0.934364	0.621110	0.378502	0.934226	0.620013	0.378138	0.934121	0.619016	0.377673	0.933735	0.617339	0.377603	0.933209	0.615745	0.377009	0.933048	0.613091	0.376541	0.932653	0.611076
H14B	0.397899	0.834277	0.653511	0.398267	0.834327	0.652965	0.397712	0.834363	0.652156	0.396997	0.834303	0.650674	0.397064	0.834073	0.649176	0.396858	0.834386	0.647678	0.395980	0.834326	0.645842
H14C	0.572162	0.892636	0.653307	0.572003	0.892833	0.652489	0.571231	0.892796	0.652145	0.570212	0.892523	0.651372	0.569656	0.892162	0.650292	0.568596	0.892453	0.649010	0.567377	0.892138	0.648094
H1A	0.718426	1.079120	-0.248107	0.718663	1.078830	-0.247771	0.718381	1.078430	-0.247420	0.718282	1.077830	-0.246773	0.718409	1.077010	-0.245932	0.718278	1.076280	-0.245012	0.718155	1.075470	-0.243806
H1B	0.703971	1.113240	-0.089785	0.703682	1.112890	-0.089537	0.703834	1.112440	-0.089178	0.703486	1.111740	-0.088588	0.703695	1.110820	-0.087835	0.703133	1.109940	-0.087014	0.703093	1.108930	-0.085754
H1C	0.879544	1.064250	-0.128588	0.879350	1.064110	-0.127990	0.879229	1.063760	-0.127941	0.878762	1.063540	-0.127234	0.878520	1.062890	-0.126459	0.877840	1.062490	-0.125457	0.877495	1.061890	-0.124289
H3	0.828682	1.074170	0.088849	0.828301	1.073840	0.089090	0.827689	1.073720	0.089485	0.827095	1.072840	0.090242	0.826307	1.072210	0.091247	0.825292	1.071330	0.092166	0.825623	1.070370	0.093208
H4	0.879210	1.019400	0.308654	0.878691	1.019180	0.308752	0.878407	1.018870	0.308769	0.877369	1.018330	0.309380	0.876200	1.017700	0.309763	0.874777	1.017030	0.310233	0.873313	1.016560	0.310844
H5	0.584213	0.864205	-0.035938	0.585042	0.864102	-0.035735	0.585669	0.864271	-0.035698	0.587596	0.864147	-0.035453	0.589179	0.864188	-0.035005	0.591188	0.864101	-0.034665	0.593107	0.864094	-0.034284
H6	0.635858	0.809956	0.182837	0.636891	0.809951	0.182519	0.637177	0.809938	0.182200	0.638742	0.810023	0.182017	0.640265	0.810067	0.181744	0.642205	0.810200	0.181474	0.643949	0.810205	0.181404
N1	0.557121	0.797842	0.444230	0.557439	0.797866	0.444108	0.557718	0.797850	0.443854	0.558259	0.797825	0.443632	0.558660	0.797866	0.443225	0.559685	0.797815	0.442921	0.560199	0.797908	0.442423
N2	0.815212	0.743304	0.417903	0.815363	0.743455	0.417910	0.815391	0.743548	0.418053	0.815324	0.743844	0.418178	0.815474	0.744176	0.418294	0.815488	0.744471	0.418633	0.815782	0.744804	0.418925
N3	0.836510	0.978870	0.576624	0.836671	0.978514	0.576632	0.836933	0.978080	0.576615	0.837198	0.977115	0.576894	0.837722	0.976138	0.576765	0.838443	0.975164	0.576921	0.838951	0.974330	0.576689
O1	0.679417	0.995101	-0.113479	0.679643	0.994971	-0.113250	0.679869	0.994797	-0.112870	0.680371	0.994433	-0.112245	0.680974	0.994061	-0.111510	0.681364	0.993665	-0.110723	0.682038	0.993358	-0.109835
O2	1.080750	0.806654	0.512495	1.080575	0.806656	0.512256	1.080503	0.806711	0.512040	1.079861	0.806590	0.511565	1.079547	0.806500	0.511233	1.079025	0.806525	0.510994	1.078474	0.806400	0.510967
O3	1.038602	0.791360	0.277544	1.038141	0.791333	0.277581	1.037766	0.791248	0.277614	1.037152	0.791189	0.277647	1.036302	0.791067	0.277835	1.035626	0.790959	0.278302	1.034989	0.790895	0.278604

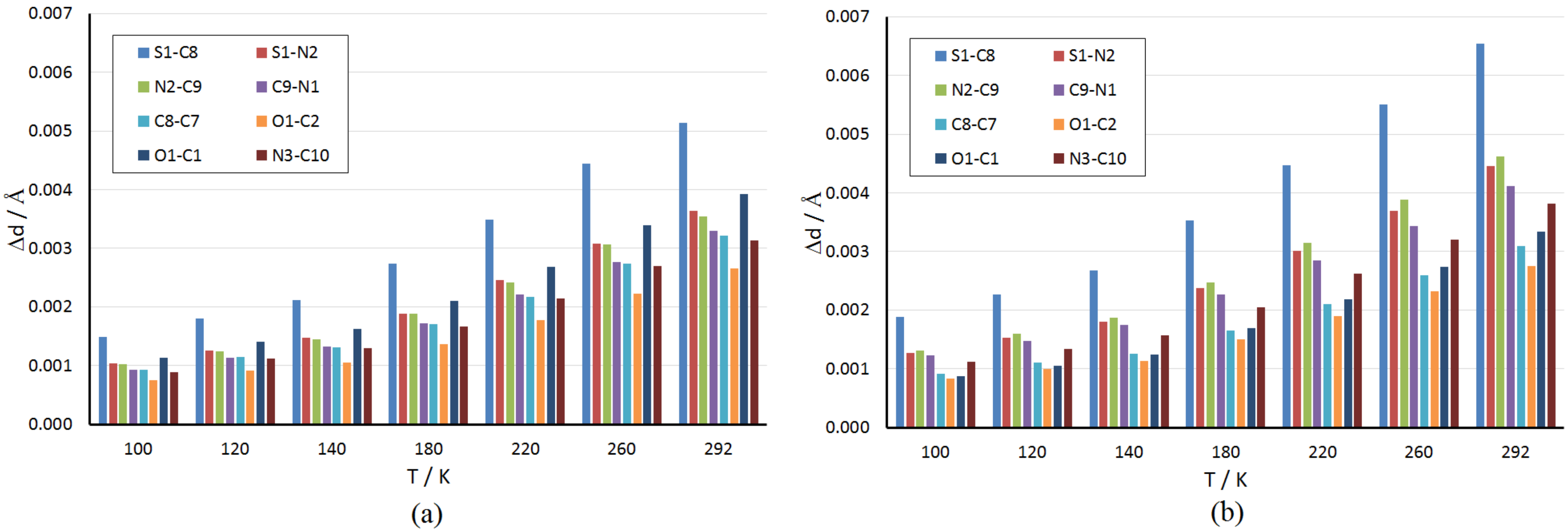

Figure S3. Change of representative covalent bond distances in DTC forms A (a, left) and B (b, right) upon application of the rigid body correction for libration motion ("TLS", see text) as a function of T. Δd is the difference between the TLS-corrected distances and the regular X-ray ones, in Å.

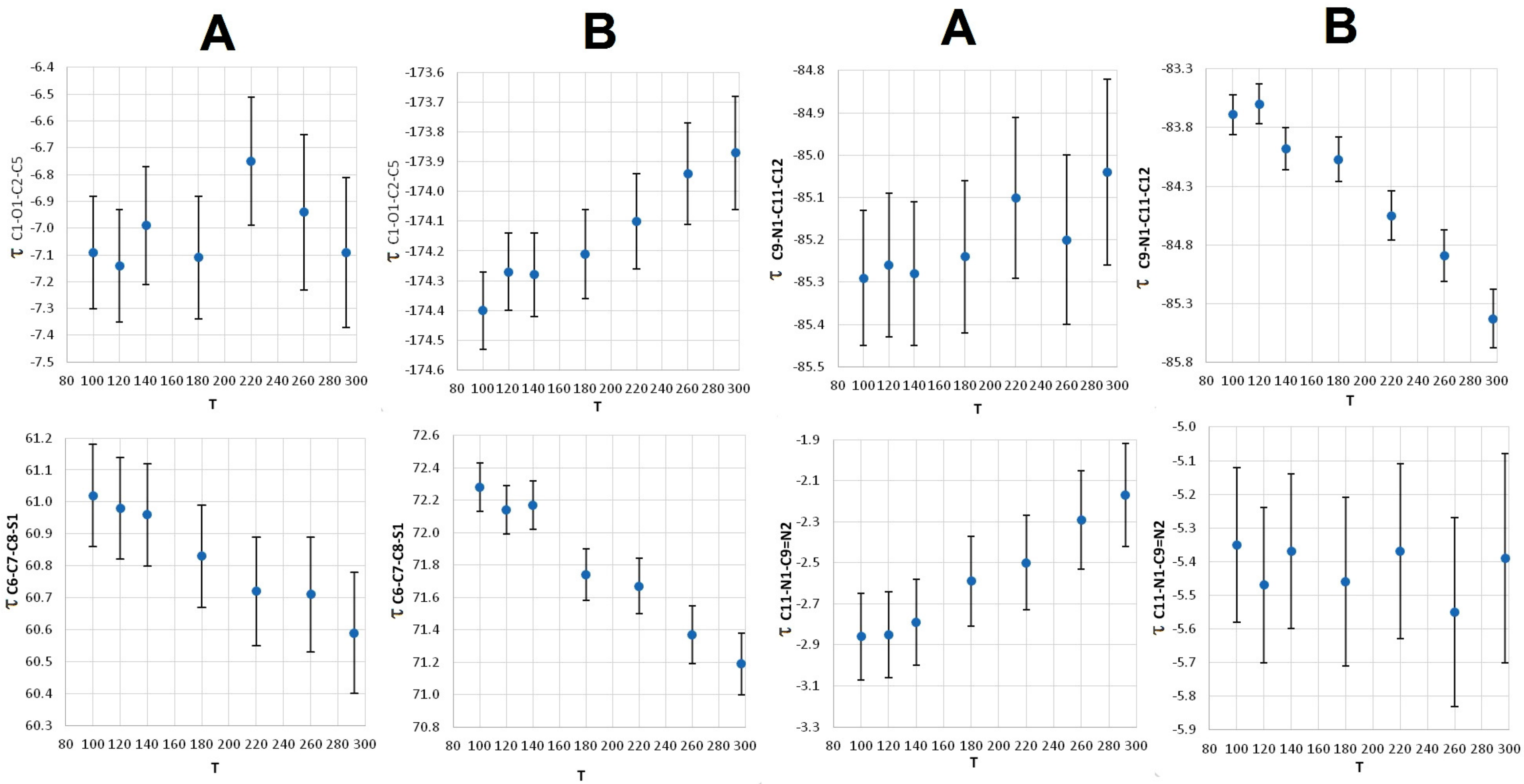

Figure S4. Behavior of selected torsion angles, τ (deg), as a function of *T* (K) in the asymmetric units of the DTC polymorphs A and B, as retrieved from the shelxl final least-square models. Vertical bars correspond to 1 estimated standard deviation. See Figure 1 in the main text for the atom numbering. The atom sequence C1–O1–C2–C5 describes the orientation of the terminal $–OCH_3$ group with respect the phenyl ring; C6–C7–C8–S1 describes how the two rings are mutually oriented; finally, C9–N1–C11–C12 and C11–N1–C9=N2 refer to the orientation of the terminal ethyl groups with respect to the thiazete ring.

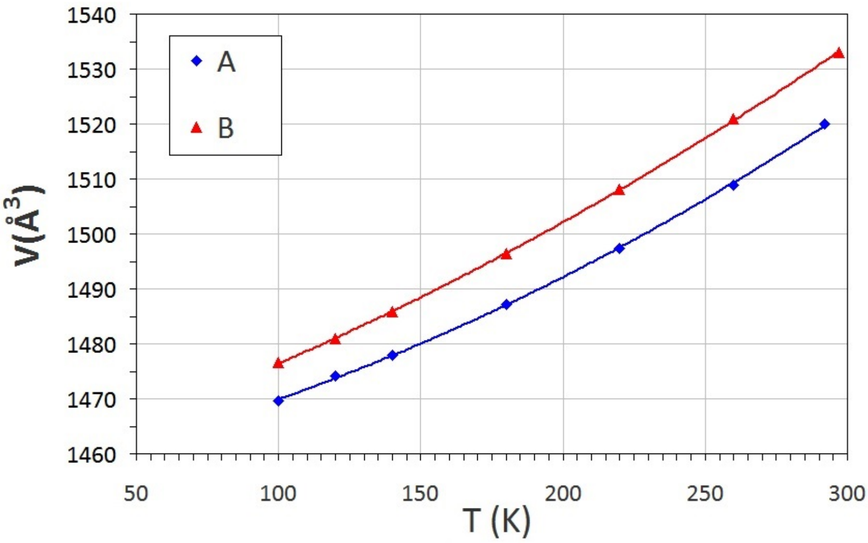

Figure S5. Cell volume (Å^3) changes affecting DTC A (blue diamonds) and B (red triangles) polymorphs as a function of *T*. The corresponding tabular data are given in Tables S1–S2 SI. Experimental average standard deviations are as low as 0.06 Å^3 for both crystal forms. Full lines derive from the linear least-squares fitting of the volume data; equations are $V(\mathrm{A}) = 4.0(4)\cdot10^{-4}\cdot T^2 + 0.10(2)\cdot T+1456(1)$ Å^3 with R^2= 0.9997 for the polymorph A and $V(\mathrm{B}) = 3.2(2)\cdot10^{-4}\cdot T^2 + 0.16(1)\cdot T+1457.1(7)$ Å^3 with R^2 = 0.9999 for the polymorph B.

S3. Crystal packing

Various CH···O and CH···N contacts ($d_{\mathrm{H\cdots O,N}} \leq 3.0$ Å, 120 deg $\leq \alpha_{\mathrm{CHO,N}} \leq$ 180 deg) are formed in A and B, even though they do not imply any obvious mono- or bi-dimensional HB network. A single CH···π contact is also present in both crystal forms, involving the H1C atom of the C1 methoxy group (Figure 1, main text) and the phenyl ring belonging to inversion-related molecules (Tables S7–S10 SI). It is questionable, however, whether these weak CH···acceptor contacts can provide truly structure-determining contributions.[18,19] For sure, most of them have poorly favorable geometries. Of the 8 and 12 intermolecular HB contacts set up in forms A and B at 100 K, 5 (A) and 9 (B) of them are significantly bent, with CH-acceptor angles in the 120-150 deg range and HB distances, in most cases, well higher than 2.5 Å. As expected (see Section 3.3 in the main text), the latter are longer in B, and this effect is even more appreciable at room temperature (Tables S8 and S10 SI). However, it is worth noting that some contacts are qualitatively conserved. With the exceptions of C3–H3···O3 and C4–H4···O2, all the HB contacts in A are also present in B among the same donor and acceptor atoms, even though the symmetry operations relating the symmetry-dependent molecules, and the corresponding bond geometries, might be different (Tables S7–S10 SI).

Table S7. Symmetry-independent CH···A (A= O, N) HB contacts in DTC form A at T = 100 K, with HB distances and angles among the following limits: 2.0 Å < $d_{H\cdots A}$ < 3.0 Å; 120 deg < $\alpha_{CH\cdots A}$ < 180 deg. The rigid-body corrected molecular geometry, with C-H distances normalized to neutron diffraction estimates (see the main text), was used to derive contact parameters (Å, deg). The reference molecule (x,y,z) corresponds to the asymmetric unit. When meaningful, estimated standard deviations (e.s.d.'s) are reported in parentheses. Different colours of the rows highlight different symmetry classes, *i.e.* white: x, y, z; blue: -x, -y, -z; green: ½-x, ½+y, ½-z; grey: ½+x, ½-y, ½+z.

Contact C–H···A	$d_{C–H}$	$d_{H\cdots A}$	$d_{C\cdots A}$	$\alpha_{CH\cdots A}$	Symmetry
C1–H1C···N2	1.077	2.967	3.799(2)	134.3	1/2-x, 1/2+y, 3/2-z
C3–H3···O3	1.083	2.585	3.611(2)	157.7	-1/2+x, 3/2-y, -1/2+z
C4–H4···O2	1.083	2.411	3.461(2)	162.9	-x, 1-y, 1-z
C5–H5···N2	1.083	2.544	3.594(2)	163.0	1/2-x, 1/2+y, 3/2-z
C6–H6···O2	1.083	2.655	3.467(2)	131.3	1/2-x, 1/2+y, 3/2-z
C12–H12B···O1	1.077	2.846	3.731(2)	139.4	1+x, y, z
C14–H14A···O3	1.077	2.827	3.614(2)	129.9	1/2+x, 3/2-y, -1/2+z
C14–H14B···N3	1.077	2.891	3.746(2)	136.5	1-x, 1-y, 1-z
C14–H14C···N3[a]	1.077	2.777	3.688(2)	142.2	x, y, z

Contact C–H···π	$d_{C–H}$	$d_{H\cdots c}$ [b]	$d_{C\cdots c}$ [b]	$\alpha_{CH\cdots c}$ [b]	$<d_{H\cdots C}>$ [c]	Symmetry
C1–H1C···*c* [b]	1.077	2.919	3.670	127.12	3.2(1)	-x, 2-y, 1-z

[a] Intramolecular contact
[b] Geometric centre of the interacting phenyl ring
[c] Average distance of the hydrogen from the carbon atoms of the phenyl ring

Table S8. Same as Table S7 above, for DTC form B at T = 100 K.

Contact C–H···A	$d_{C–H}$	$d_{H\cdots A}$	$d_{C\cdots A}$	$\alpha_{CH\cdots A}$	Symmetry
C1–H1B···N2	1.077	2.879	3.920(2)	162.7	3/2-x, 1/2+y, 1/2-z
C4–H4···N3	1.083	2.544	3.407(2)	136.0	2-x, 2-y, 1-z
C5–H5···N2	1.083	2.904	3.821(2)	142.6	-1/2+x, 3/2-y, -1/2+z
C6–H6···O2	1.083	2.691	3.446(2)	126.5	-1/2+x, 3/2-y, -1/2+z
C11–H11A···O2	1.092	2.807	3.714(2)	140.3	-1+x, y, z
C12–H12A···O1	1.077	2.784	3.845(2)	168.6	-1/2+x, 3/2-y, 1/2+z
C12–H12B···O3	1.077	2.709	3.642(2)	144.8	-1+x, y, z
C12–H12C···O2	1.077	2.722	3.577(2)	136.1	-1/2+x, 3/2-y, -1/2+z
C13–H13A···O2	1.092	2.560	3.373(2)	130.6	-1+x, y, z
C13–H13A···O3	1.092	2.994	4.054(2)	163.7	-1+x, y, z
C14–H14A···N3	1.077	2.999	3.772(2)	129.0	1-x, 2-y, 1-z
C14–H14B···O3	1.077	2.728	3.527(2)	130.7	-1/2+x, 3/2-y, 1/2+z
C14–H14C···N3 [a]	1.077	2.817	3.630(2)	132.3	x, y, z

Contact C–H···π	$d_{C–H}$	$d_{H\cdots c}$ [b]	$d_{C\cdots c}$ [b]	$\alpha_{CH\cdots c}$ [b]	$<d_{H\cdots C}>$ [c]	Symmetry
C1–H1C···*c* [b]	1.077	3.210	4.270	168.3	3.5(2)	2-x, 2-y, -z

[a] Intramolecular contact
[b] Geometric centre of the interacting phenyl ring
[c] Average distance of the hydrogen from the carbon atoms of the phenyl ring

Table S9. Same as Table S7 above, for DTC form A at RT. To the sake of comparison, the same contacts are shown, no matter they fulfill the above described geometrical cutoffs.

Contact C–H···A	$d_{C–H}$	$d_{H···A}$	$d_{C···A}$	$\alpha_{CH···A}$	Symmetry
C1–H1C···N2	1.077	3.000	3.851(3)	136.2	1/2-x, 1/2+y, 3/2-z
C3–H3···O3	1.083	2.721	3.749(2)	158.2	-1/2+x, 3/2-y, -1/2+z
C4–H4···O2	1.083	2.482	3.527(2)	161.8	-x, 1-y, 1-z
C5–H5···N2	1.083	2.607	3.648(2)	161.1	1/2-x, 1/2+y, 3/2-z
C6–H6···O2	1.083	2.738	3.535(2)	130.2	1/2-x, 1/2+y, 3/2-z
C12–H12B···O1	1.077	2.967	3.833(3)	137.7	1+x, y, z
C14–H14A···O3	1.077	2.885	3.695(3)	132.1	1/2+x, 3/2-y, -1/2+z
C14–H14B···N3	1.077	2.947	3.805(3)	137.0	1-x, 1-y, 1-z
C14–H14C···N3[a]	1.077	2.776	3.691(3)	142.7	x, y, z

Contact C–H···π	$d_{C–H}$	$d_{H···c}$ [b]	$d_{C···c}$ [b]	$\alpha_{CH···c}$ [b]	$<d_{H···C}>$ [c]	Symmetry
C1–H1C···c [b]	1.077	3.020	3.732	124.1	3.3(1)	-x, 2-y, 1-z

[a] Intramolecular contact
[b] Geometric centre of the interacting phenyl ring
[c] Average distance of the hydrogen from the carbon atoms of the phenyl ring

Table S10. Same as Table S7 above, for DTC form B at RT.

Contact C–H···A	$d_{C–H}$	$d_{H···A}$	$d_{C···A}$	$\alpha_{CH···A}$	Symmetry
C1–H1B···N2	1.077	2.968	4.005(3)	161.9	3/2-x, 1/2+y, 1/2-z
C3–H3···N2	1.083	3.017	3.924(3)	141.6	-1/2+x, 3/2-y, -1/2+z
C4–H4···O2	1.083	2.738	3.513(3)	128.3	-1/2+x, 3/2-y, -1/2+z
C6–H6···N3	1.083	2.594	3.459(3)	136.3	2-x, 2-y, 1-z
C11–H11A···O2	1.092	2.911	3.809(3)	138.1	-1+x, y, z
C12–H12A···O1	1.077	2.860	3.921(3)	168.5	-1/2+x, 3/2-y, 1/2+z
C12–H12B···O3	1.077	2.781	3.719(3)	145.5	-1+x, y, z
C12–H12C···O2	1.077	2.747	3.610(3)	136.9	-1/2+x, 3/2-y, -1/2+z
C13–H13A···O2	1.092	2.665	3.458(2)	129.1	-1+x, y, z
C13–H13A···O3	1.092	3.050	4.118(2)	165.8	-1+x, y, z
C14–H14A···N3	1.077	3.027	3.853(3)	133.9	1-x, 2-y, 1-z
C14–H14B···O3	1.077	2.799	3.601(3)	131.2	-1/2+x, 3/2-y, 1/2+z
C14–H14C···N3 [a]	1.077	2.850	3.675(4)	133.5	x, y, z

Contact C–H···π	$d_{C–H}$	$d_{H···c}$ [b]	$d_{C···c}$ [b]	$\alpha_{CH···c}$ [b]	$<d_{H···C}>$ [c]	Symmetry
C1–H1C···c [b]	1.077	3.258	4.314	166.8	3.5(2)	2-x, 2-y, -z

[a] Intramolecular contact
[b] Geometric centre of the interacting phenyl ring
[c] Average distance of the hydrogen from the carbon atoms of the phenyl ring

Table S11. Lattice parameters[a] of the real (A/A and B/B) and virtual (A/B and B/A) DTC polymorphs, generated upon the full optimization at the M06/86–311G**(sulphur)+6–31G*(other atoms) theory level at T = 0 K. All the optimizations were carried out under the same $P2_1/n$ symmetry constraints of the real DTC lattices. The corresponding cohesive energies and densities are shown in Table 1 (main text).

Lattice / Conformer	A/A	B/B	A/B	B/A
a / Å	8.24841975	8.05643312	8.02397280	8.15368535
b / Å	13.15257490	16.41263278	12.82074608	16.56378038
c / Å	12.57967799	10.09740146	13.15513339	10.48158244
β / deg	95.639858	94.796244	93.739757	90.166433
V / Å^3	1358.137235	1330.476669	1350.430474	1415.593090

[a] We provide in this Table as many figures as possible to facilitate comparisons with future theoretical calculations. Figures over three digits after the comma should be dropped for comparison with experimental results.

Table S12. Total cohesive energy per molecule for the A and B DTC polymorphs as a function of T, as computed by M06/*pob*-TZVP quantum simulation of the various crystal structures at their experimental geometries. Corrections for molecular relaxation and basis set superposition error were applied (see the main text for full details). In the last column, the point-by-point differences between the A and B forms are also reported. All values are given in kcal·mol^{-1}.

T/K	Form A	Form B	Δ
100	-19.18	-16.96	-2.21
120	-18.96	-16.68	-2.28
140	-18.76	-16.53	-2.23
180	-18.33	-15.94	-2.39
220	-17.73	-15.27	-2.46
260	-17.13	-14.35	-2.78
RT	-16.41	-13.78	-2.63

Table S13. As Table S12 above, from PBE0+D/*pob*-TZVP estimates.

T/K	Form A	Form B	Δ
100	40.62	40.71	-0.09
120	40.61	40.72	-0.11
140	40.47	40.51	-0.04
180	40.47	40.37	0.10
220	40.38	40.30	0.09
260	40.18	40.39	-0.21
RT	40.16	40.23	-0.07

S4. Molecule-molecule interaction energies

While discussing results on the energy decomposition, it should be taken into account that any partition of energy eigenvalues – the true observables – into terms trying to describe specific physical effects, always comes with many ifs and buts.[20,21] This is even truer when NCI energy terms are estimated by means of semiempirical methods. As often occurs in polymorphic structures,[22,23] the energy difference between the two crystal forms of the title compound is low (see Section 3.6 in the main text), while the individual electrostatic, dispersive and repulsive contributions are always up to an order of magnitude higher (see Section 3.8 in the main text). Thus, reproducing even the correct energy ranking of the two DTC forms using semiempirical functionals is rather tricky. With this *caveat* in mind, we first checked the ability of different computational methods to reproduce all-electron M06/*pob*–TZVP pairwise molecule-molecule interaction energies, E_{int} (Section 2.6 in the main text), as a function of their centre-of-mass distance in both A and B forms at $T = 100$ K (Figure S6).

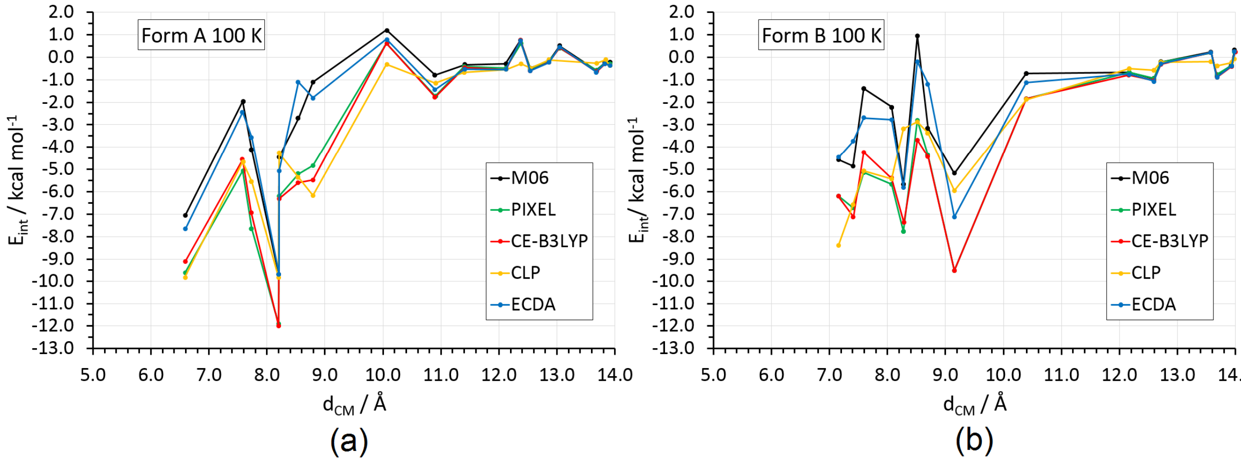

Figure S6. Interaction energies, E_{int} (kcal·mol^{-1}), for DTC molecular pairs extracted from the crystal at their experimental (TLS+H)-corrected geometries, as a function of the center of mass distance, d_{CM} (Å) at T=100 K. Results ECDA (blue) are shown. Broken lines serve just as guides for the eye. See Sections 2.7 and S1 SI for full details on the ECDA functional. (a) Form A. (b) Form B.

From figure S6, it is clear that the A form bears a couple of particularly stable molecular pairs (E_{int} = –7.1 and –9.7 kcal·mol^{-1}) at short centre of mass distances (d_{CM} = 6.59 and 8.21 Å, black curves in Figure S6). The most attractive pairs in B are instead shifted at less negative E_{int}'s (–5.7 and –5.2 kcal·mol^{-1}) and larger centre-of-mass separations (d_{CM} = 8.28 and 9.15 Å). This complies well with the predicted higher stability of polymorph A (Section 3.6 in the main text). In general, all the methods show a good qualitative agreement to the general trends of M06/*pob*-TZVP interaction energies (Figure S6). The only exception is the fully empirical and computationally inexpensive AA-CLP recipe (yellow curve), which fails to correctly predict relative energies at low centre of mass separations, especially in the polymorph B. As expected, CE-B3LYP and PIXEL outcomes are quite similar, as they share various aspects of their parametrization. In most cases, they reproduce the correct ranking of molecular pairs, even though they both tend to produce slightly more negative interaction energies. The ECDA curve (Sections 2.7 and S1 SI) is much closer to the M06 reference, the corresponding root mean square deviations (RMSD) being 0.54 kcal·mol^{-1} (form A) and 0.93 kcal·mol^{-1} (form B). For the sake of comparison, PIXEL and CE-B3LYP estimates bear larger RMSD with respect to M06: ~1.8 kcal·mol^{-1} (form A) and ~2.1 kcal·mol^{-1} (form B).

It is out of the scope of the present work to assess critically pros and cons of the various energy decomposition schemes here explored; a complete study would require considering other classes of molecular crystals, due to the very peculiar nature**Errore. Il segnalibro non è definito.** of DTC. Rather, we are interested in finding general conclusions, independent from the specific computational recipe used to compute individual energy terms. To this end, Figure S7 compares the individual electrostatic (E_{el}) and dispersive-repulsive ($E_{dr} = E_{dis} + E_{rep}$) contributions to E_{int}, as a function of both the centre-of-mass distance and the computational method for the three methods in close agreement with M06 energies.

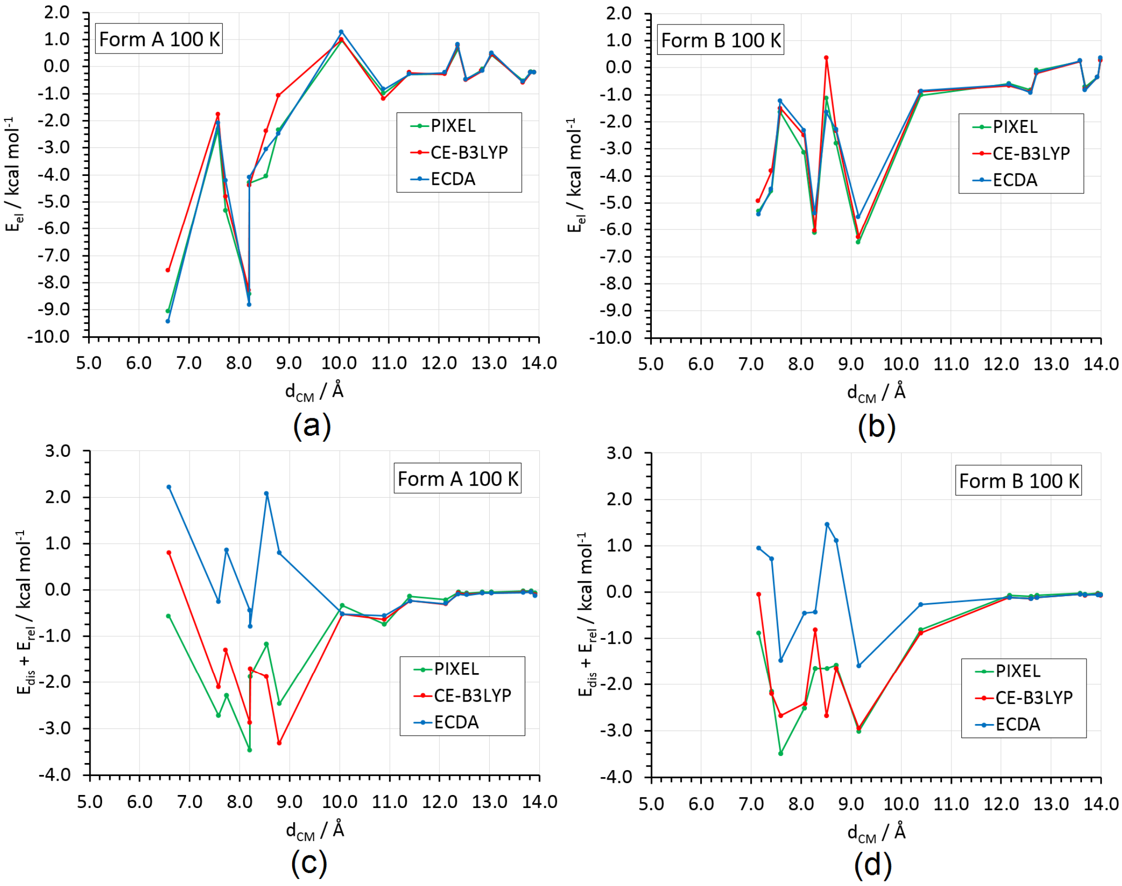

Figure S7. (a-b) Electrostatic contributions, $E_{el} = E_c + E_p$, to E_{int} as a function of d_{CM} (Å) from different energy decomposition schemes. green: PIXEL; red: CE-B3LYP; blue: ECDA. (a) Form A. (b) Form B. (c-d) Same as (a-b), for the dispersive-repulsive balance, $E_{dr} = E_{dis}+E_{rep}$. (c) Form A. (d) Form B. All values are given in kcal·mol^{-1}.

The first take-home message from Figure S7 is that the electrostatic terms at short d_{CM} are up to two or three times more negative than the dispersive-repulsive ones. Accordingly, trends of total interaction energy, E_{int}, closely follow the behaviour of E_{el} in both polymorphs (compare the curves in Figure S6 with those in Figure S7a,b). In other words, electrostatics is dominating in determining interaction energetics of neighbouring pairs in these crystals. Second, there is a remarkable conformity of views among CE-B3LYP, PIXEL and ECDA procedures in estimating E_{el}. On the contrary, the dispersive-repulsive contributions are more prone to depend on the specific computational approach and are predicted to be significantly less negative in the framework of the ECDA model (Figure S7c,d). The very good agreement with M06/*pob*–TZVP estimates for E_{int} (Figure S6, black and blue curves) is due to the fact that ECDA electrostatic terms are computed on the basis of the same M06/*pob*–TZVP wavefunctions. Some kind of error compensation operating on the dispersive-repulsive part of the functional cannot be also excluded. In any case, the ECDA results shown in Figures S7–S8 can be considered as a reasonably good approximation of our quantum predictions for interaction energetics in DTC.

Table S14. ECDA WYSK/WY/RZR (see Section S1) decomposition into electrostatic (E_{el}), dispersion (E_{dis}) and repulsion (E_{rep}) terms of the total cohesive energy per molecule of A (first row) and B (second row) polymorphs of DTC as a function of T. All values are given in kcal·mol^{-1}.

T / K	E_{el}	E_{rep}	E_{dis}	E_{coh}
100	-12.26	20.05	-19.98	-12.19
	-11.34	17.61	-18.89	-12.62
120	-12.10	19.68	-19.81	-12.23
	-11.19	17.24	-18.72	-12.66
140	-11.02	16.89	-18.54	-12.67
	-11.02	16.89	-18.54	-12.67
180	-11.55	18.52	-19.30	-12.33
	-10.67	16.11	-18.15	-12.71
220	-11.18	17.72	-18.92	-12.38
	-10.32	15.32	-17.74	-12.74
260	-10.78	16.82	-18.49	-12.45
	-9.95	14.49	-17.30	-12.76
RT	-10.40	16.02	-18.10	-12.48
	-9.61	13.74	-16.89	-12.75

References

[1] S. P. Thomas, P. R. Spackman, , D. Jayatilaka and M. A. Spackman, *J. Chem. Theory Comput*., 2018, **14**, 1614.
[2] M. A. Spackman and D. Jayatilaka, *CrystEngComm*, 2009, **11**, 19
[3] A. Gavezzotti, CLP User's manual, 2016. Manual, executables, and source codes are freely available at http://www.angelogavezzotti.it.
[4] A. Gavezzotti, *J. Phys. Chem. B,* 2003, **107**, 2344.
[5] M. J. Frisch, G. W. Trucks, H. B. Schlegel, G. E. Scuseria, M. A. Robb, J. R. Cheeseman, G. Scalmani, V. Barone *et al*., *Gaussian 09 (Revision A.1)*, 2009, Gaussian, Inc., Wallingford CT.
[6] A. Gavezzotti, CLP User's manual, 2016. Manual, executables, and source codes are freely available at http://www.angelogavezzotti.it
[7] M. Barzaghi, *PAMoC (Version 2010–07–27), Online User's Manual*; CNR–ISTM, Institute of Molecular Science and Technologies: Milano, Italy; URL: www.istm.cnr.it/~barz/pamoc/.
[8] M. A. Spackman, *Chem Phys. Lett*., 2006, **418**, 158.
[9] M. A. Spackman, Keynote Lecture KN23.28, *Electrostatic and related properties from accurate charge density analyses,* IUCR2005, Book of Abstracts; Firenze; 2005; C5.
[10] A. D. Buckingham, *Physical Chemistry: An Advanced Treatise*; ed. D. Henderson, Academic Press: New York, 1970; 349.
[11] J. C. Slater and J. G. Kirkwood, *Phys. Rev*. ,1931, **37**, 682.
[12] Q. Wu and W.Yang, *J. Chem. Phys*., 2002, **116**, 515.
[13] T. P. Haley, E. R. Graybill and S. M. Cybulski, *J. Chem. Phys*., 2006, **124**, 204301.
[14] K. T.Tang and J. P. Toennies, *J. Chem. Phys*. 1984, **80**, 3726.
[15] S. Grimme, *J. Comput. Chem.,* 2004, **25**, 1463.
[16] M. A. Spackman, *J. Chem. Phys*.,1986, **85**, 6579.
[17] T. Ziegler and A. Rauk, *Theoretica Chimica Acta*, 1977, **46**, 1.
[18] A. Gavezzotti and L. Lo Presti, *Cryst. Growth Des*. 2016, **16**, 2952.
[19] L. Lo Presti, *CrystEngComm,* 2018, Advance article. DOI: 10.1039/c8ce00674a.
[20] R. F. W. Bader, *Chemistry – A European Journal*, 2006, **12**, 2896.
[21] F. Cortés–Guzmán and R. F. W. Bader, *Coordination Chemistry Reviews*, 2005, **249**, 633.
[22] A. Gavezzotti, V. Colombo and L. Lo Presti, *Crystal Growth Des*., 2016, **16**, 6095.
[23] , V. Colombo, L. Lo Presti and A. Gavezzotti, *CrystEngComm*, 2017, **19**, 2413.